

Fast Lithium Ion Diffusion in Brownmillerite $\text{Li}_x\text{Sr}_2\text{Co}_2\text{O}_5$

Xin Chen,¹ Xixiang Zhang,² Jie-Xiang Yu,^{1,3,*} and Jiadong Zang³

¹*School of Physical Science and Technology, Soochow University, Suzhou 215006, China*

²*Physical Science and Engineering Division, King Abdullah University of*

Science and Technology (KAUST), Thuwal 23955-6900, Kingdom of Saudi Arabia

³*Department of Physics and Astronomy, University of New Hampshire, Durham, New Hampshire 03824, USA*

Ionic conductors have great potential for interesting tunable physical properties via ionic liquid gating and novel energy storage applications such as all-solid-state lithium batteries. In particular, low migration barriers and high hopping attempt frequency are the keys to achieve fast ion diffusion in solids. Taking advantage of the oxygen-vacancy channel in $\text{Li}_x\text{Sr}_2\text{Co}_2\text{O}_5$, we show that migration barriers of lithium ion are as small as 0.28 ~ 0.17 eV depending on the lithium concentration rates. Our first-principles calculation also investigated hopping attempt frequency and concluded the room temperature ionic diffusivity and ion conductivity is high as $10^{-7} \sim 10^{-6} \text{ cm}^2 \text{ s}^{-1}$ and $10^{-3} \sim 10^{-2} \text{ S} \cdot \text{cm}^{-1}$ respectively, which outperform most of perovskite-type, garnet-type and sulfide Li-ion solid-state electrolytes. This work proves $\text{Li}_x\text{Sr}_2\text{Co}_2\text{O}_5$ as a promising solid-state electrolyte.

I. INTRODUCTION

Ionic diffusion in solids has played a key role in not only manipulating many interesting physical properties in ion-electron-lattice-coupled systems via ionic liquid gating (ILG)[1–3], but also great potential applications in energy storage such as all-solid-state lithium batteries in which solid electrolytes with both high Li-ion conductivity and low electron conductivity[4, 5]. To achieve highly efficient ionic diffusion, high ion conductivity or high ionic diffusivity is required. According to Nernst-Einstein equation[6, 7], the relationship between ionic diffusivity D and ion conductivity σ_i in solids can be given by

$$\sigma_i = q^2 n D \beta \quad (1)$$

where q is the electric charge of conducting ion, n is the ionic carrier concentration and $\beta = (k_B T)^{-1}$ is the Boltzmann factor, the inverse of the product of Boltzmann constant and temperature. Meanwhile, under kinetically ideal conditions, the diffusivity can also be described by ion hopping through a pathway with a hopping frequency via Vogeles-Tammann-Fulcher model[8], which is given by

$$D = a^2 \nu^* \exp(-E_a \beta) \quad (2)$$

where a is the hopping distance between two neighbor stable sites, ν^* is the hopping attempt frequency and E_a is the activation energy of ions or the migration barriers during the diffusion. To this end, the high hopping attempt frequency and the low migration barriers is crucial for fast ionic diffusion.

Perovskite-type oxide systems are promising candidates for all-solid-state lithium batteries due to their well ordered diffusion channels and the high Young's modulus[9]. Furthermore, the desirable combination of the complex electron-lattice-spin coupling, the strongly correlated d -electrons and the multivalent transition metal ions in transition metal oxides

brings about novel electronic and magnetic properties[10–12]. Similar to the perovskite-type oxides, the recent study on brownmillerite $\text{Sr}_2\text{Co}_2\text{O}_5$ demonstrated that ILG could induce tri-state phase transformation from $\text{Sr}_2\text{Co}_2\text{O}_5$ to perovskite SrCoO_3 and $\text{H}_2\text{Sr}_2\text{Co}_2\text{O}_5$ by the insertion of oxygen anions and hydrogen cations respectively[2]. Han *et al.*[13] also reported that the direction of the oxygen-vacancy channels can be well controlled. The well-ordered[14] and controllable oxygen-vacancy channels in brownmillerite $\text{Sr}_2\text{Co}_2\text{O}_5$ provide favorable conditions for fast ionic diffusion and storage of ions, bringing about applications in fuel cells and rechargeable batteries.

In this paper, we systemically studied the diffusion of Li^+ ion in brownmillerite $\text{Sr}_2\text{Co}_2\text{O}_5$ based on first-principles calculations. The injected Li^+ cations can be stabilized inside the oxygen-vacancy channels to form $\text{Li}_x\text{Sr}_2\text{Co}_2\text{O}_5$ ($x = 0.0 \sim 1.0$). After confirming the chemical stability, we obtained the migration barrier of Li^+ cations along the oxygen-vacancy channels as 0.28 ~ 0.17 eV Li^+ depending on Li^+ concentration rates. The low migration barrier is caused by the multi-bonding property of Li-O bonds, and is lower than most of the Perovskite-type Li-ion solid electrolytes. The corresponding diffusivity and conductivity at room temperature are obtained as $10^{-7} \sim 10^{-6} \text{ cm}^2 \text{ s}^{-1}$ and $10^{-3} \sim 10^{-2} \text{ S} \cdot \text{cm}^{-1}$ respectively. Such high ionic diffusivity and ion conductivity can be considered as a super-ionic conductor[15].

II. METHODOLOGY

We performed density-functional theory (DFT) based calculations with projector augmented wave pseudopotentials[16, 17] implemented in the Vienna ab initio simulation (VASP) package[18, 19]. The generalized gradient approximation in Perdew, Burke, and Ernzerhof formation[20] was used as the exchange-correlation energy and the Hubbard U method[21] ($U = 5.0 \text{ eV}$, $J = 0.9 \text{ eV}$) was applied on Co($3d$) orbitals to include strong-correlation effects. An energy cutoff of 600 eV was used for the plane-wave expansion throughout the calculations. The k -points

* jxyu@suda.edu.cn

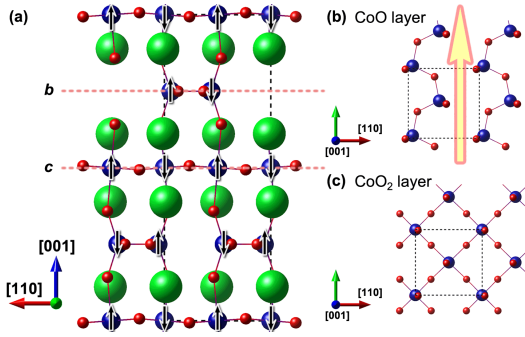


Figure 1. Crystal structure of $\text{Sr}_2\text{Co}_2\text{O}_5$ in one unit cell. (a) The side view along $[\bar{1}10]$ direction. Blue, red and green balls represent Co, O and Sr atoms respectively. The top view of the CoO layer and the CoO_2 layer in b and c are shown in (b) and (c) respectively. Black arrows in (a) shows the G-AFM spin-ordering and the yellow arrow in (b) indicates the vacancy channel along the $[\bar{1}10]$ direction in the CoO layer.

were sampled on a $10 \times 10 \times 4$ Monkhorst-Pack mesh in the Brillouin zone of the unit cell of $\text{Sr}_2\text{Co}_2\text{O}_5$ containing eight Co, eight Sr and twenty O atoms. For structural relaxations we relaxed the atoms until the Hellmann-Feynman forces were less than $1 \text{ meV}/\text{\AA}$.

In order to find the diffusion path and the corresponding migration barriers for Li diffusion in $\text{Li}_x\text{Sr}_2\text{Co}_2\text{O}_5$, we performed climbing image nudged elastic band (cl-NEB) calculations[22, 23] to find the saddle point and the minimum energy path between two stable local minimum. Eight images were employed and the force convergence is down to $0.02 \text{ eV}/\text{\AA}$. Phonon modes of the diffused Li^+ ions were obtained by using the finite displacement method[24] implemented in the Phonopy package[25].

III. STRUCTURAL, ELECTRONIC AND MAGNETIC PROPERTIES OF $\text{Sr}_2\text{Co}_2\text{O}_5$

Structure – The atomic structure of $\text{Sr}_2\text{Co}_2\text{O}_5$ is shown in Fig. 1. It has orthorhombic symmetry with space group $Pma2$ (28). Compared to a $\sqrt{2} \times \sqrt{2} \times 4$ perovskite supercell of SrCoO_3 , the unit cell of $\text{Sr}_2\text{Co}_2\text{O}_5$ loses four O atoms with two CoO layers (b in Fig. 1(a)) appearing. CoO layers shown in Fig. 1(b) have more spacing than CoO_2 layers Fig. 1(c). Periodic oxygen-vacancy channel structures are formed along the $[\bar{1}10]$ direction so that they can provide the well-ordered diffusion channels marked in Fig. 1(b). The lattice constant for the orthorhombic unit cell with eight cobalt atoms, namely $(\text{Sr}_2\text{Co}_2\text{O}_5)_4$ is $a = 5.57 \text{ \AA}$, $b = 5.46 \text{ \AA}$, and $c = 16.00 \text{ \AA}$.

Electronic and magnetic properties – The total energy results show that $\text{Sr}_2\text{Co}_2\text{O}_5$ has the ground state with G-type antiferromagnetic (G-AF) or rocksalt-type antiferromagnetism (AFM) spin ordering, consistent with previous studies[14]. G-AF is 68 meV per Co lower in energy than C-type AFM (C-AF) or column-type AFM, 101 meV lower than A-type AFM (A-AF) or layered-type AFM and 142 meV lower than ferromagnetic (FM) ordering. Therefore, the electronic structure of

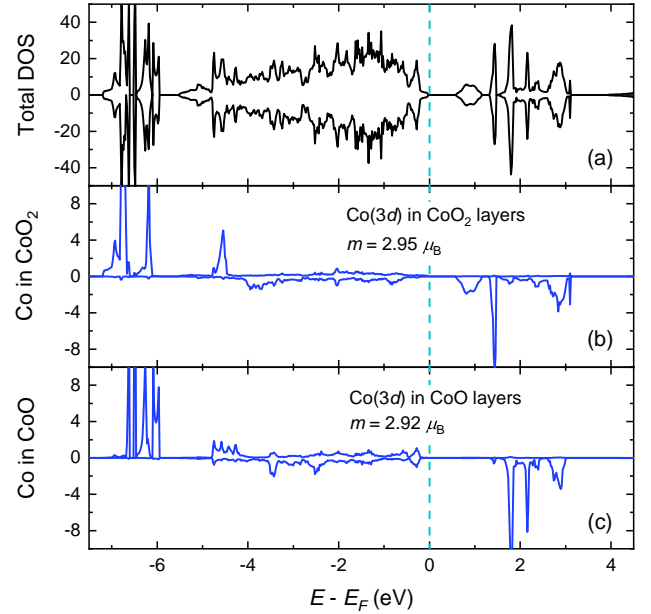


Figure 2. In the unit cell of $(\text{Sr}_2\text{Co}_2\text{O}_5)_4$ under G-AF ordering, (a) the total density-of-state (DOS) and the projected DOS (PDOS) of $\text{Co}(3d)$ in (b) CoO_2 layers and in (c) CoO layers. Positive and negative values represent the spin-majority (spin-up) and spin-minority (spin-down) channels respectively. The Fermi level is set to zero. The local spin magnetic moment on Co is also listed.

$\text{Sr}_2\text{Co}_2\text{O}_5$ with G-AF ordering is investigated. According to the density-of-state (DOS) result shown in Fig. 2, a band gap about 0.6 eV indicates its insulating. In $\text{Sr}_2\text{Co}_2\text{O}_5$, Co cations have valence state $+3$ with six d electrons (d^6) in principle, so that the high-spin state of Co^{3+} is $S = 2$ which should have $4.0 \mu_B$ local magnetic moment with five spin-majority and one spin-minority d electrons. According to PDOS result in Fig. 2(b)(c), The featured $\text{Co}(3d)$ in both CoO_2 and CoO layers are all below the Fermi level in the spin-up channel, indicating Co's are indeed in the high-spin state. However, the local moment obtained by DFT is only $2.95 \mu_B$. According to the on-site density matrices and the corresponding occupancy of both two types of Co, six orbitals - five in spin-majority and one in spin-minority - are fully occupied with occupancy closed to 1, while other four orbitals have occupancy $0.12 \sim 0.48$, indicating unoccupied $3d$ orbitals but hybridized with oxygen ligands under the ligand field. Such high Co-O hybridization leads to $\text{Co}^{2+}\underline{L}$ state where the underline \underline{L} refers to a ligand hole[14, 26]. To this end, d^6 configuration with $S = 2$ high spin state on all Co^{3+} is still justified.

IV. LITHIUM-INJECTED $\text{Li}_x\text{Sr}_2\text{Co}_2\text{O}_5$

We now investigated the situations where Li atoms are injected into $\text{Sr}_2\text{Co}_2\text{O}_5$. With one Li placed in the unit cell, the most stable structure of $\text{Li}_{0.25}\text{Sr}_2\text{Co}_2\text{O}_5$ is shown in Fig. 3. One Li atom is located in the spacing of a CoO layer, at a hol-

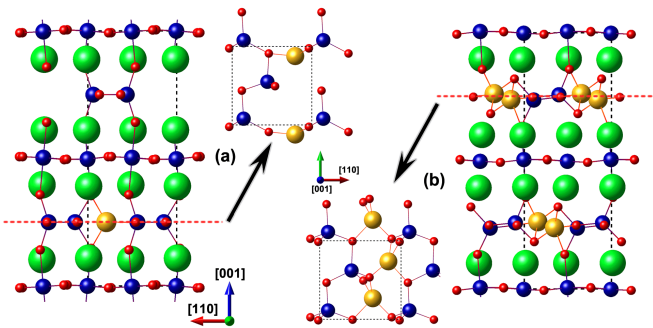


Figure 3. Crystal structures of (a) $\text{Li}_{0.25}\text{Sr}_2\text{Co}_2\text{O}_5$ with one Li atoms (yellow balls) per unit cell placed and (b) $\text{LiSr}_2\text{Co}_2\text{O}_5$ with four Li atoms per unit cell placed in side views and top views. The dashed lines in side views are the CoO layers for top views.

low site in the center of the oxygen-vacancy channel and have bonds with surrounding four O atoms. It is distinct from the protonated $\text{H}_x\text{Sr}_2\text{Co}_2\text{O}_5$ where each injected H^+ cation is located next to an oxygen atom with a strong O – H bond so that H^+ cations are not in the same plane with CoO layers[2, 27]. Thus, it is obvious that at most four Li atoms can be placed into a $(\text{Sr}_2\text{Co}_2\text{O}_5)_4$ unit cell to form $\text{LiSr}_2\text{Co}_2\text{O}_5$, where all injected Li^+ cations are located in the oxygen-vacancy channels, shown in Fig.3. The lattice constant for $\text{LiSr}_2\text{Co}_2\text{O}_5$ are $a = 5.72 \text{ \AA}$, $b = 5.50 \text{ \AA}$ and $c = 16.75 \text{ \AA}$, only about 8% expansion in volume. The chemical stability can be confirmed by the formation energy of $\text{Li}_x\text{Sr}_2\text{Co}_2\text{O}_5$ from bulk $\text{Sr}_2\text{Co}_2\text{O}_5$ and Lithium metal, which is defined by

$$E_f = E_{\text{Li}_n(\text{Sr}_2\text{Co}_2\text{O}_5)_4} - nE_{\text{Li}} - E_{(\text{Sr}_2\text{Co}_2\text{O}_5)_4} \quad (3)$$

where $n = 4x$ is the number of Li placed in the $(\text{Sr}_2\text{Co}_2\text{O}_5)_4$ unit cell and the total energy for face-centered cubic Li lattice is used for E_{Li} .

The formation energy results for $n = 1, 3, 4$ are -2.01 , -5.60 and -7.98 eV per unit cell respectively. Those for all three non-equivalent $n = 2$ situations are -2.93 , -3.20 and -3.74 eV respectively. They are all negative, indicating the system reduce energy when $\text{Li}_x\text{Sr}_2\text{Co}_2\text{O}_5$ formed with the injected Li atoms. The injected Li atoms can be stabilized in the oxygen-vacancy channels in all the cases of various concentration rates.

To investigate how lithium's injection affect the electronic structure and magnetic ordering, we therefore focus on $\text{LiSr}_2\text{Co}_2\text{O}_5$ with all four hollow sites in the unit cell occupied by Li atoms to maximum the effect. Since each Li^+ cation has valence state +1, the average valence state of Co is +2.5. In that case, half of Co are +3 with d^6 and half are +2 with d^7 . G-AF spin ordering with zero net magnetization still has the lowest total energy so that four Co ions in the unit cell has spin-up local spin magnetic moment and other four are spin-down. The corresponding DOS and PDOS on four spin-up Co ions labeled Co1, Co2, Co3 and Co4 are shown in Fig.4. The total DOS gives a band gap about 0.8 eV indicating the insulating properties. The local spin magnetic moments, Co1 and Co2 in CoO_2 layers are $1.83 \mu_B$ and $2.73 \mu_B$ respectively, and those on Co3 and Co4 in CoO layers are $1.83 \mu_B$ and $2.73 \mu_B$

respectively. According to PDOS results of Co, Co1(3d) in CoO_2 layers (Fig. 4(b)) has unoccupied states above the Fermi level in the spin-up channel, indicating that Co1 is not in the high spin state. On the other hand, a sharp peak appears around -4.5eV below the Fermi level in the spin-down channel, indicating that Co1 has more occupied state in the spin-down channel than Co^{3+} in $\text{Sr}_2\text{Co}_2\text{O}_5$. Co2(3d) in CoO_2 layers (Fig.4(c)) and Co3(3d) in CoO layers (Fig.4(d)) has fully occupied state in the spin-up channel while in the spin-down channel, the unoccupied state is located around $3.0 \sim 4.0\text{eV}$ above the Fermi level, 1.0 eV higher than the unoccupied state of Co^{3+} in $\text{Sr}_2\text{Co}_2\text{O}_5$. It indicates that d electrons on Co2 and Co3 in $\text{LiSr}_2\text{Co}_2\text{O}_5$ meet stronger on-site Coulomb interaction with more d electrons than on Co^{3+} in $\text{Sr}_2\text{Co}_2\text{O}_5$. PDOS of Co4 in CoO layers (Fig.4(e)) are similar to that of Co in $\text{Sr}_2\text{Co}_2\text{O}_5$.

We still examined the onsite density matrices and the corresponding occupancies of all the four types of Co ions. For Co1 in CoO_2 layers, four orbitals in spin-majority and two in spin-minority are occupied with occupancies close to 1, and others have occupancies $0.12 \sim 0.48$, indicating unoccupied 3d orbitals which only have hybridization bonding-states with the surrounding oxygen ligands. Therefore, Co1 has +3 valence state and d^6 configuration with $S = 1$ intermediate spin state. For Co2 in CoO_2 layers and Co3 in CoO layers, five orbitals in spin-majority and two in spin-minority are occupied with occupancies close to 1, so that they are both in +2 valence state and d^7 configuration with $S = 3/2$ high spin state. For Co4 in CoO layers, five orbitals in spin-majority and one in spin-minority are occupied with occupancies close to 1, so that Co4 are in +3 valence state and d^6 configuration with $S = 2$ high spin state. The insulating properties and the G-AF spin ordering ground state are also confirmed in the electronic structures of $\text{Li}_x\text{Sr}_2\text{Co}_2\text{O}_5$ with $x = 0.25, 0.5$ and 0.75 . Due to the multivalent cobalt cations, Li^+ -injection $\text{Li}_x\text{Sr}_2\text{Co}_2\text{O}_5$ does not affect the insulating properties and the antiferromagnetic ordering.

V. DIFFUSION PROPERTIES OF LI IN $\text{Li}_x\text{Sr}_2\text{Co}_2\text{O}_5$

To investigate the diffusion of Li^+ cations in $\text{Li}_x\text{Sr}_2\text{Co}_2\text{O}_5$, we first calculated the migration barriers of Li^+ cations with various Li concentration x in $\text{Li}_x\text{Sr}_2\text{Co}_2\text{O}_5$. With one Li atom in the unit cell, $\text{Li}_{0.25}\text{Sr}_2\text{Co}_2\text{O}_5$ mimics the situation where very few Li^+ cations are injected in the $\text{Sr}_2\text{Co}_2\text{O}_5$. We set two stable structural configuration as the initial and ending states and other eight intermediate images on the diffusion pathway are used to find the lowest migration barriers using cl-NEB calculations. The results are shown in Fig.5. The migration barrier is 0.28 eV at the saddle point state with highest potential energy (c in Fig.5). We also calculated the migration barrier of a Li^+ cation with three Li atoms in the unit cell, that is $\text{Li}_{0.75}\text{Sr}_2\text{Co}_2\text{O}_5$. This simulates the opposite situation where Li^+ cations occupy most of the hollow sites in the oxygen-vacancy channels. The carriers is the "holes" by analogy with hole carriers in the p-doping electronic semiconductors. The results are shown in Fig.6. The migration barrier is 0.17eV

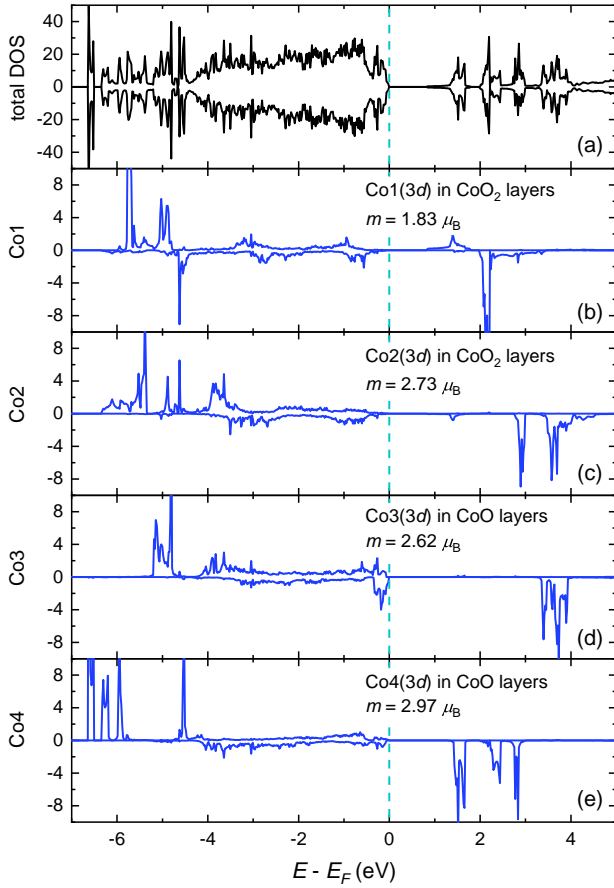


Figure 4. In the unit cell of $(\text{LiSr}_2\text{Co}_2\text{O}_5)_4$ in G-AF ordering, (a) the total DOS and the PDOS of $3d$ orbitals of Co1, Co2, Co3 and Co4 which is the four Co atoms with positive local spin magnetic moments in the unit cell.

where the saddle point state is c in Fig.6. The two cases cover the two most common situations for ionic diffusion. According to the side-views of each image, in both two cases, the diffusion pathways are all along the oxygen-vacancy channels. This magnitude of migration barrier is similar with or even lower than that of H^+ diffusion in the protonated $\text{H}_x\text{Sr}_2\text{Co}_2\text{O}_5$ (~ 0.3 eV)[27]. It is also significantly lower than most of the migration barriers of the perovskite-type Li-ion solid electrolytes ($0.6 \sim 0.2$ eV)[9].

To obtain the origin of the low migration barriers of $\text{Li}_x\text{Sr}_2\text{Co}_2\text{O}_5$, we investigated the bonding properties between Li and O during the diffusion. As mentioned, four Li-O bonds are established for each Li^+ at the initial state. During the diffusion, two of the four bonds still remains and the other two bonds are broken to form two new bonds near the ending state. Fig.7 shows the charge differences between intermediate/ending states and the initial state for $\text{Li}_{0.25}\text{Sr}_2\text{Co}_2\text{O}_5$ and $\text{Li}_{0.75}\text{Sr}_2\text{Co}_2\text{O}_5$ respectively. The change of the spatial charge distribution illustrates the change of the chemical bonds during the diffusion. For both cases, while the old bonds are being broken, the new bonds have been created in the saddle point state (c-a in Fig.7(a) and (b)). The newly formed bonds com-

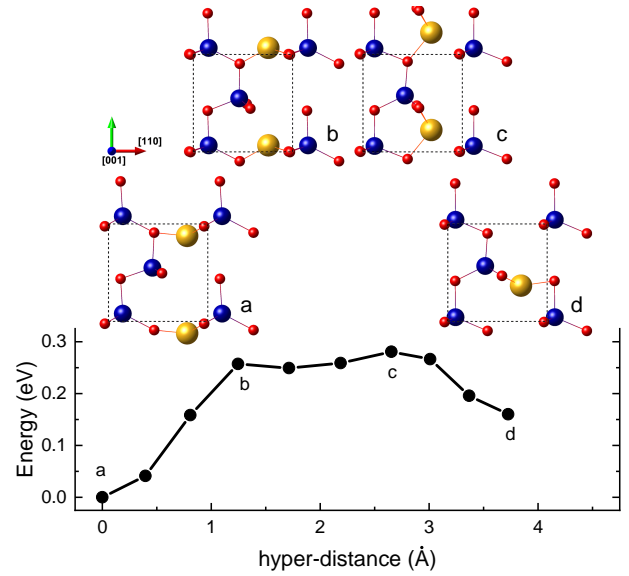


Figure 5. cl-NEB results of one Li diffusion in the unit cell of $\text{Li}_{0.25}\text{Sr}_2\text{Co}_2\text{O}_5$. The diagram is the total energies of each state relative to the initial state as a function of hyper-distances between each intermediate image and the initial state. a-d show the top view of the intermediate images labeled in the diagram.

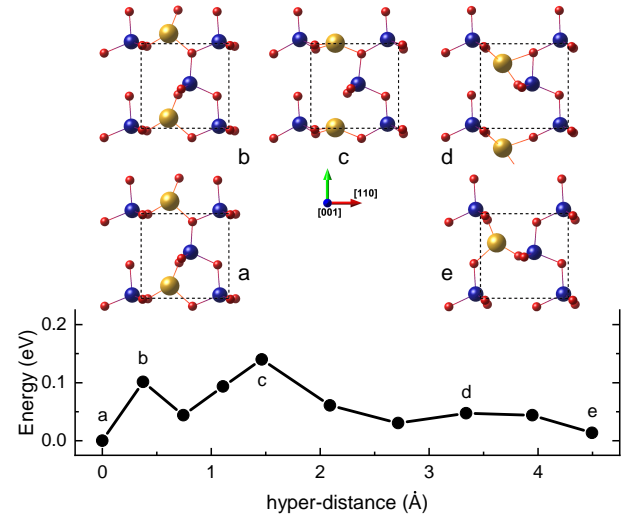


Figure 6. NEB results of one Li diffusion in the unit cell of $\text{Li}_{0.75}\text{Sr}_2\text{Co}_2\text{O}_5$. a-e show the top views of the intermediate images labeled in the diagram.

pensate the energy cost of broken bonds, eventually reducing the migration barriers.

The ionic diffusivity/conductivity in a solid depends not only on the migration barriers but also on the pre-exponential factor $a^2\nu^*$ in Eq.2. According to Vineyard formula[28, 29], the hopping attempt frequency can be given by

$$\nu^* = \frac{\prod_{i=1}^N \nu_i^0}{\prod_{j=1}^{N-1} \nu_j^s} \quad (4)$$

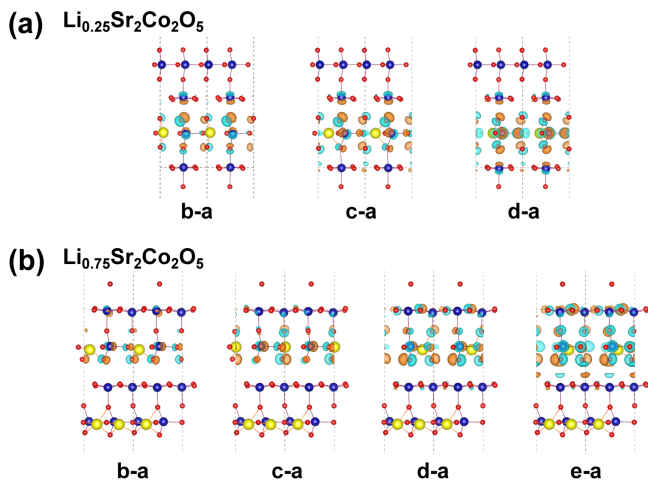


Figure 7. In the side views, the charge differences between initial state (labeled a) and intermediate/ending states (labeled b-d for $\text{Li}_{0.25}\text{Sr}_2\text{Co}_2\text{O}_5$ and b-e for $\text{Li}_{0.75}\text{Sr}_2\text{Co}_2\text{O}_5$) for (a) $\text{Li}_{0.25}\text{Sr}_2\text{Co}_2\text{O}_5$ and (b) $\text{Li}_{0.75}\text{Sr}_2\text{Co}_2\text{O}_5$. The labels corresponds to the label in Fig.5 and Fig.6. Orange and cyan isosurfaces correspond to positive and negative values respectively.

where ν_i^0 and ν_j^s are the normal frequencies at the Γ point of vibration modes of the initial and saddle point state, respectively. Notice that the number of normal modes in the product of saddle point is one less than that in initial state. That is because of the presence of an imaginary frequencies mode at the saddle point state caused by the instability along the diffusion direction. This mode needs to be removed from the product. The phonon modes at the Γ point for the initial and the saddle point state of both $\text{Li}_{0.25}\text{Sr}_2\text{Co}_2\text{O}_5$ and $\text{Li}_{0.75}\text{Sr}_2\text{Co}_2\text{O}_5$ were therefore calculated. As a result, the hopping attempt frequencies for $\text{Li}_{0.25}\text{Sr}_2\text{Co}_2\text{O}_5$ and $\text{Li}_{0.75}\text{Sr}_2\text{Co}_2\text{O}_5$ are 6.87 THz and 0.95 THz, respectively. The lower migration barrier usually leads to a smoother potential energy surface for diffusion, causing the lower force constant and the corresponding vibration frequency. So that the hopping attempt frequency for $\text{Li}_{0.75}\text{Sr}_2\text{Co}_2\text{O}_5$ is lower than that for $\text{Li}_{0.25}\text{Sr}_2\text{Co}_2\text{O}_5$. The hopping distance is regarded as the half of the lattice constant along $[\bar{1}10]$ direction, which is $2.75 \times 10^{-8}\text{cm}$ for both two phases. To this end, for $\text{Li}_{0.25}\text{Sr}_2\text{Co}_2\text{O}_5$ and $\text{Li}_{0.75}\text{Sr}_2\text{Co}_2\text{O}_5$, we can estimate the pre-exponential factor of diffusivity $a^2\nu^*$, which is $5.20 \times 10^{-3}\text{cm}^2\text{s}^{-1}$ and $0.72 \times 10^{-3}\text{cm}^2\text{s}^{-1}$ respectively. The hopping attempt frequency can be regarded

as the frequency that the diffused ions attempt to climb over the barrier, so that $\nu^* \exp(-E_a/k_B T)$ is nothing but the hopping frequency from one stable site to its neighbor site with a successful hopping. At room temperature with $T = 300\text{K}$, $\beta = k_B T = 38.7\text{eV}^{-1}$, the ionic diffusivity D based on Vogel-Tammann-Fulcher model (Eq.2) is $1.02 \times 10^{-7}\text{cm}^2\text{s}^{-1}$ and $1.00 \times 10^{-6}\text{cm}^2\text{s}^{-1}$ respectively. If the ionic concentration n is regarded as one Li^+ cation per unit cell, the corresponding ionic conductivity $\sigma_i = q^2 n D \beta$ based on Eq.1 are therefore $1.20 \times 10^{-3}\text{S}\cdot\text{cm}^{-1}$ and $1.17 \times 10^{-2}\text{S}\cdot\text{cm}^{-1}$ respectively. The room temperature diffusivity and conductivity are both superior to most of the perovskite-type Li-ion solid electrolytes ($10^{-4} \sim 10^{-3}\text{S}\cdot\text{cm}^{-1}$ for bulk conductivity)[9], garnet-type solid-state electrolytes ($10^{-4} \sim 10^{-3}\text{S}\cdot\text{cm}^{-1}$)[30], and sulfide solid electrolytes ($10^{-7} \sim 10^{-3}\text{S}\cdot\text{cm}^{-1}$)[31].

VI. CONCLUSIONS

In summary, We investigated the structural, electronic and magnetic properties of brownmillerite $\text{Li}_x\text{Sr}_2\text{Co}_2\text{O}_5$ and confirmed the oxygen vacancy channels, the insulating property and the G-AF spin ordering ground state. At most four Li^+ cations can be stabilized in the center of the oxygen vacancy channels of an orthorhombic $(\text{Sr}_2\text{Co}_2\text{O}_5)_4$ unit cell to form $\text{Li}_x\text{Sr}_2\text{Co}_2\text{O}_5$ ($x = 0.0 \sim 1.0$). The G-AF spin ordering and insulating property is still remained with the lithium's injection. By employing cl-NEB calculations, we obtained the migration barriers of $\text{Li}_x\text{Sr}_2\text{Co}_2\text{O}_5$ for $x = 0.25$ and 0.75 as 0.28 eV and 0.17 eV, respectively. After obtaining the hopping attempt frequencies via Vineyard formula, we therefore obtained the corresponding diffusivity and conductivity at the room temperature as $1.02 \times 10^{-7}\text{cm}^2\text{s}^{-1}$ and $1.20 \times 10^{-3}\text{S}\cdot\text{cm}^{-1}$ for $x = 0.25$ respectively, and $1.00 \times 10^{-6}\text{cm}^2\text{s}^{-1}$ and $1.17 \times 10^{-2}\text{S}\cdot\text{cm}^{-1}$ for $x = 0.75$ respectively. The high ionic diffusivity and ion conductivity indicate brownmillerite $\text{Sr}_2\text{Co}_2\text{O}_5$ as a promising super-ionic conductor.

ACKNOWLEDGMENTS

We are grateful for fruitful discussions with Prof. Pu Yu. This work was financially supported by the National Natural Science Foundation of China (12274309). The cl-NEB calculations were performed at Shaheen II in King Abdullah University of Science and Technology (KAUST).

[1] A. J. Tan, M. Huang, C. O. Avci, F. Büttner, M. Mann, W. Hu, C. Mazzoli, S. Wilkins, H. L. Tuller, and G. S. D. Beach, *Nature Materials* **18**, 35 (2018).

[2] N. Lu, P. Zhang, Q. Zhang, R. Qiao, Q. He, H.-B. Li, Y. Wang, J. Guo, D. Zhang, Z. Duan, Z. Li, M. Wang, S. Yang, M. Yan, E. Arenholz, S. Zhou, W. Yang, L. Gu, C.-W. Nan, J. Wu, Y. Tokura, and P. Yu, *Nature* **546**, 124 (2017).

[3] Z. Li, S. Shen, Z. Tian, K. Hwangbo, M. Wang, Y. Wang, F. M. Bartram, L. He, Y. Lyu, Y. Dong, G. Wan, H. Li, N. Lu, J. Zang, H. Zhou, E. Arenholz, Q. He, L. Yang, W. Luo, and P. Yu, *Nature Communications* **11**, 184 (2020).

[4] Y. Wang, B. Liu, Q. Li, S. Cartmell, S. Ferrara, Z. D. Deng, and J. Xiao, *Journal of Power Sources* **286**, 330 (2015).

[5] D. Aksyonov, A. Boev, S. Fedotov, and A. Abakumov, *Solid State Ionics* **393**, 116170 (2023).

- [6] R. Kutner, *Physics Letters A* **81**, 239 (1981).
- [7] M. Park, X. Zhang, M. Chung, G. B. Less, and A. M. Sastry, *Journal of Power Sources* **195**, 7904 (2010).
- [8] M. Ikeda and M. Aniya, *Journal of Non-Crystalline Solids* **371-372**, 53 (2013).
- [9] J. Lu and Y. Li, *Journal of Materials Science: Materials in Electronics* **32**, 9736 (2021).
- [10] M. Imada, A. Fujimori, and Y. Tokura, *Reviews of Modern Physics* **70**, 1039 (1998).
- [11] E. Dagotto, *Science* **309**, 257 (2005).
- [12] J. Ngai, F. Walker, and C. Ahn, *Annual Review of Materials Research* **44**, 1 (2014).
- [13] H. Han, A. Sharma, H. L. Meyerheim, J. Yoon, H. Deniz, K.-R. Jeon, A. K. Sharma, K. Mohseni, C. Guillemard, M. Valvidares, P. Gargiani, and S. S. P. Parkin, *ACS Nano* **16**, 6206 (2022).
- [14] A. Muñoz, C. de la Calle, J. A. Alonso, P. M. Botta, V. Pardo, D. Baldomir, and J. Rivas, *Physical Review B* **78**, 054404 (2008).
- [15] X. He, Y. Zhu, and Y. Mo, *Nature Communications* **8**, 15893 (2017).
- [16] P. E. Blöchl, *Physical Review B* **50**, 17953 (1994).
- [17] G. Kresse and D. Joubert, *Physical Review B* **59**, 1758 (1999).
- [18] G. Kresse and J. Furthmüller, *Computation Materials Science* **6**, 15 (1996).
- [19] G. Kresse and J. Furthmüller, *Physical Review B* **54**, 11169 (1996).
- [20] J. P. Perdew, K. Burke, and M. Ernzerhof, *Physical Review Letters* **77**, 3865 (1996).
- [21] A. I. Liechtenstein, V. I. Anisimov, and J. Zaanen, *Physical Review B* **52**, R5467 (1995).
- [22] G. Henkelman, B. P. Uberuaga, and H. Jónsson, *The Journal of Chemical Physics* **113**, 9901 (2000).
- [23] G. Henkelman and H. Jónsson, *The Journal of Chemical Physics* **113**, 9978 (2000).
- [24] K. Parlinski, Z. Q. Li, and Y. Kawazoe, *Physical Review Letters* **78**, 4063 (1997).
- [25] A. Togo and I. Tanaka, *Scripta Materialia* **108**, 1 (2015).
- [26] M. A. Korotin, S. Y. Ezhov, I. V. Solovyev, V. I. Anisimov, D. I. Khomskii, and G. A. Sawatzky, *Physical Review B* **54**, 5309 (1996).
- [27] N. Lu, Y. Wang, S. Qiao, H.-B. Li, Q. He, Z. Li, M. Wang, J. Zhang, S. C. Tsang, J. Guo, S. Yang, J. Zhang, K. Deng, D. Zhang, J. Ma, Y. Wu, J. Zhu, Y. Tokura, C.-W. Nan, J. Wu, and P. Yu, A protonated brownmillerite electrolyte for superior low-temperature proton conductivity (2018), [arXiv:1811.10802 \[cond-mat.mtrl-sci\]](https://arxiv.org/abs/1811.10802).
- [28] G. H. Vineyard, *Journal of Physics and Chemistry of Solids* **3**, 121 (1957).
- [29] J. Koettgen, T. Zacherle, S. Grieshammer, and M. Martin, *Physical Chemistry Chemical Physics* **19**, 9957 (2017).
- [30] C. Wang, K. Fu, S. P. Kammampata, D. W. McOwen, A. J. Samson, L. Zhang, G. T. Hitz, A. M. Nolan, E. D. Wachsmann, Y. Mo, V. Thangadurai, and L. Hu, *Chemical Reviews* **120**, 4257 (2020).
- [31] A. Manthiram, X. Yu, and S. Wang, *Nature Reviews Materials* **2**, 16103 (2017).